

# PROMIDIS $\alpha$ : A T-cell receptor $\alpha$ signature associated with immunodeficiencies caused by V(D)J recombination defects



Aurélien Berland, BSc,<sup>a,b,\*</sup> Jérémie Rosain, PharmD,<sup>b,c,\*</sup> Sophie Kaltenbach, PharmD, PhD,<sup>a,b,\*</sup> Vincent Allain, MD,<sup>c</sup> Nizar Mahlaoui, MD, MSc,<sup>b,d</sup> Isabelle Melki, MD,<sup>d,e</sup> Alice Fievet, MD, MSc,<sup>f,g</sup> Catherine Dubois d'Enghien, BSc,<sup>g</sup> Marie Ouachée-Chardin, MD, PhD,<sup>h</sup> Laurence Perrin, MD,<sup>i</sup> Nathalie Auger, MD,<sup>j</sup> Funda Erol Cipe, MD,<sup>k</sup> Andrea Finocchi, MD, PhD,<sup>l</sup> Figen Dogu, MD,<sup>m</sup> Felipe Suarez, MD, PhD,<sup>n</sup> Despina Moshous, MD, PhD,<sup>a,b,d</sup> Thierry Leblanc, MD,<sup>h</sup> Alexandre Belot, MD, PhD,<sup>o</sup> Claire Fieschi, MD, PhD,<sup>p</sup> David Boutboul, MD, PhD,<sup>p</sup> Marion Malphettes, MD,<sup>p</sup> Lionel Galicier, MD,<sup>p</sup> Eric Oksenhendler, MD, PhD,<sup>p</sup> Stéphane Blanche, MD,<sup>d</sup> Alain Fischer, MD, PhD,<sup>b,c,q,r</sup> Patrick Revy, PhD,<sup>a,b</sup> Dominique Stoppa-Lyonnet, MD, PhD,<sup>f,g,s</sup> Capucine Picard, MD, PhD,<sup>b,c</sup> and Jean-Pierre de Villartay, PhD<sup>a,b</sup>

Paris, Villejuif, and Lyon, France; Istanbul and Ankara, Turkey; and Rome, Italy

**Background:** V(D)J recombination ensures the diversity of the adaptive immune system. Although its complete defect causes severe combined immunodeficiency (ie, T<sup>+</sup>B<sup>+</sup> severe combined immunodeficiency), its suboptimal activity is associated with a broad spectrum of immune manifestations, such as late-onset combined immunodeficiency and autoimmunity. The earliest molecular diagnosis of these patients is required to adopt the best therapy strategy, particularly when it involves a myeloablative conditioning regimen for hematopoietic stem cell transplantation. **Objective:** We aimed at developing biomarkers based on analysis of the T-cell receptor (TCR)  $\alpha$  repertoire to assist in the diagnosis of patients with primary immunodeficiencies with V(D)J recombination and DNA repair deficiencies.

**Methods:** We used flow cytometric (fluorescence-activated cell sorting) analysis to quantify TCR-V $\alpha$ 7.2-expressing T lymphocytes in peripheral blood and developed PROMIDIS $\alpha$ , a multiplex RT-PCR/next-generation sequencing assay, to evaluate a subset of the TCR $\alpha$  repertoire in T lymphocytes. **Results:** The combined fluorescence-activated cell sorting and PROMIDIS $\alpha$  analyses revealed specific signatures in patients with V(D)J recombination-defective primary immunodeficiencies or ataxia telangiectasia/Nijmegen breakage syndromes. **Conclusion:** Analysis of the TCR $\alpha$  repertoire is particularly appropriate in a prospective way to identify patients with partial immune defects caused by suboptimal V(D)J

recombination activity, a DNA repair defect, or both. It also constitutes a valuable tool for the retrospective *in vivo* functional validation of variants identified through exome or panel sequencing. Its broader implementation might be of interest to assist early diagnosis of patients presenting with hypomorphic DNA repair defects inclined to experience acute toxicity during prehematopoietic stem cell transplantation conditioning. (J Allergy Clin Immunol 2019;143:325-34.)

**Key words:** Primary immunodeficiency, V(D)J recombination, T-cell receptor  $\alpha$  repertoire, ataxia telangiectasia, DNA repair, next-generation sequencing

The adaptive immune system is composed of B and T lymphocytes that express immune receptors, immunoglobulins, and T-cell receptors (TCRs), respectively, presenting a diversity allowing the subject to face any antigens. This plasticity is ensured by V(D)J recombination, a somatic DNA rearrangement process that results in the combinatorial association of previously dispersed variable (V), diversity (D), and joining (J) gene segments, which form the immune recognition moiety of immunoglobulins and TCRs.<sup>1</sup> Briefly, V(D)J recombination is initiated by lymphoid-specific factors encoded by recombination-activating gene 1 (*RAG1*) and *RAG2* through introduction of a

From "Laboratory "Genome Dynamics in the Immune System," INSERM UMR1163, Paris; <sup>b</sup>Université Paris Descartes Sorbonne Paris Cité, Institut Imagine, Paris; <sup>c</sup>the Study Center for Primary Immunodeficiencies, Necker-Enfants Malades Hospital, Assistance Publique Hôpitaux de Paris (APHP), Necker Medical School, Paris; <sup>d</sup>the Pediatric Immuno-Haematology and Rheumatology Unit, Necker Enfants Malades University Hospital, Assistance Publique-Hôpitaux de Paris, Paris; <sup>e</sup>General Pediatrics, Infectious Disease and Internal Medicine Department, Hôpital Robert Debré, (APHP), Paris; <sup>f</sup>INSERM U830 and <sup>g</sup>Service de Génétique, Institut Curie, Paris; <sup>h</sup>the Department of Pediatric Hematology, Robert-Debré (APHP), Paris; <sup>i</sup>the Department of Genetics, Robert Debré Hospital, (APHP), Paris; <sup>j</sup>the Department of Biopathology, Institut Gustave Roussy, Villejuif; <sup>k</sup>the Department of Pediatric Allergy-Immunology, Kanuni Sultan Suleyman Research and Training Hospital, Istanbul; <sup>l</sup>DPUO, University Department of Pediatrics, Bambino Gesù Children's Hospital and University of Tor Vergata School of Medicine, Rome; <sup>m</sup>the Department of Pediatric Immunology and Allergy, Ankara University School of Medicine; <sup>n</sup>the Department of Haematology, Necker-Enfants Malades University Hospital, (APHP), Paris; <sup>o</sup>Pediatric Rheumatology, Nephrology and Dermatology Department, Hôpital Femme-Mère-Enfant, Hospices civils de Lyon; <sup>p</sup>the Department of Clinical

Immunology, Hôpital Saint-Louis, (APHP), Paris; <sup>q</sup>INSERM UMR1163, Paris; <sup>r</sup>Collège de France, Paris; and <sup>s</sup>Université Paris Descartes Sorbonne Paris Cité, Paris.

\*These authors contributed equally to this work.

Supported by institutional grants from INSERM and the Agence Nationale de la Recherche (ANR-13-PRTS-0004) and by grants from La Ligue Nationale contre le Cancer (Equipe Labellisée LA LIGUE 2017) and the AT-Europe Foundation.

Disclosure of potential conflict of interest: The authors declare that they have no relevant conflicts of interest.

Received for publication November 20, 2017; revised April 17, 2018; accepted for publication May 25, 2018.

Available online June 12, 2018.

Corresponding author: Jean-Pierre de Villartay, PhD, DGS, "Equipe Labellisée Ligue Contre le Cancer", INSERM UMR1163, Institut Imagine, 24 bd du Montparnasse, 75015 Paris, France. E-mail: devillartay@gmail.com.

The CrossMark symbol notifies online readers when updates have been made to the article such as errata or minor corrections

0091-6749/\$36.00

© 2018 American Academy of Allergy, Asthma & Immunology  
<https://doi.org/10.1016/j.jaci.2018.05.028>

**Abbreviations used**

AT:	Ataxia telangiectasia
ATM:	Ataxia telangiectasia mutated
CID:	Combined immunodeficiency disease
CVID:	Common variable immunodeficiency
DCLRE1C:	DNA cross-link repair 1C/Artemis
FACS:	Fluorescence-activated cell sorting
KO:	Knockout
NBN:	Nibrin
NBS:	Nijmegen breakage syndrome
NGS:	Next-generation sequencing
NK:	Natural killer
PBL:	Peripheral blood lymphocyte
PCA:	Principal component analysis
PGM:	Personal Genome Machine
PID:	Primary immunodeficiency
PRKDC:	Protein kinase, DNA-activated, catalytic polypeptide
RAG:	Recombination-activating gene
ROR $\gamma$ T:	RAR-related orphan receptor $\gamma$ T
SCID:	Severe combined immunodeficiency
SMART:	Switching mechanism at the 5'-end of the RNA transcript
TCR:	T-cell receptor
TRAJ:	T-cell receptor $\alpha$ joining gene
TRAV:	T-cell receptor $\alpha$ variable gene
XLF:	XRCC4-like factor

DNA double-strand break at the border of the rearranging segments (see Schatz and Swanson<sup>2</sup> for a review). The DNA double-strand break is then processed and repaired by the ubiquitously expressed DNA repair machinery of the cell based on the nonhomologous DNA end-joining pathway (see Alt et al<sup>3</sup> for a review).

Since the genes coding for RAG1/2 factors were cloned, generation of deficient animal models and analyses of patients with severe combined immunodeficiency (SCID) lacking T and B lymphocytes (T<sup>-</sup>B<sup>-</sup> natural killer [NK]<sup>+</sup> SCID) clearly established the absolute requirement of these factors and the V(D)J recombination machinery as a whole for proper maturation of adaptive immune cells.<sup>4</sup> Nevertheless, a broad spectrum of immunodeficiencies was described subsequently that was associated with hypomorphic mutations in *RAG1/2* genes that spare some V(D)J recombination activity (for a recent review, see Notarangelo et al<sup>5</sup>). The phenotype of these patients extends from the very severe Omenn syndrome condition characterized by an oligoclonal expansion of activated T lymphocytes that infiltrate the gut and skin to milder conditions, such as late-onset combined immune deficiency with granuloma and/or various autoimmune manifestations. The clinical severity appears to be a function of RAG residual activity and hence extension of TCR repertoire diversity in these patients.<sup>6,7</sup> RAG deficiency was also identified as a possible cause of agammaglobulinemia, isolated T CD4 lymphopenia, common variable immunodeficiency (CVID), isolated IgA deficiency, hyper-IgM syndrome, and even sterile chronic multifocal osteomyelitis.<sup>5</sup> In addition to mutations in *RAG* genes, defects in the DNA repair phase of the V(D)J recombination alter generation of a diversified adaptive immune system. Consequences can be severe, ranging from T<sup>-</sup>B<sup>-</sup>NK<sup>+</sup> SCID when associated with null mutations in *Artemis* or *Cernunnos* genes to almost asymptomatic in some cases of hypomorphic mutations in, for example, DNA ligase IV.<sup>4</sup>

Various degrees of immunodeficiency are also associated with other DNA repair defect conditions, such as ataxia telangiectasia (AT) with mutations in the ataxia telangiectasia mutated (*ATM*) gene,<sup>8</sup> or Nijmegen breakage syndrome (NBS) harboring mutations in the nibrin gene (*NBN*),<sup>9</sup> the formal diagnosis of which is often difficult in young children in the absence of fully developed clinical signs of the disease. Thus it is crucial to benefit from robust experimental tools to help distinguish the various possible molecular causes underlying these immune-deregulated conditions. The early diagnosis of DNA repair defects is also of critical importance because hematopoietic stem cell transplantation is often the only curative treatment and because these patients can have acute toxicity after administration of DNA damage-inducing drugs used for conditioning regimens.<sup>10</sup>

Based on our prior observations of a bias in the TCR $\alpha$  repertoire in patients with *Cernunnos* mutations and XRCC4-like factor (*Xlf*) knockout (KO) mice,<sup>11</sup> we aimed to develop biomarkers that would help in the diagnosis of suboptimal V(D)J recombination conditions, as well as DNA repair defects. Here we present the combination of fluorescence-activated cell sorting (FACS) analysis and PROMIDIS $\alpha$ , an RT-PCR/next-generation sequencing (NGS)-based resource, to analyze a subset of the TCR $\alpha$  repertoire that distinctly reveals patients with V(D)J recombination anomalies and proved very robust in the early diagnosis of AT and NBS conditions.

## METHODS

### Patients and control subjects

For V $\alpha$ 7.2 analysis using FACS, the healthy control cohort was studied between January 2017 and March 2017. It included 16 children aged 0 to 18 years with no suspicion of primary immunodeficiency (PID) or immunosuppressive treatment and 17 healthy adult subjects (age, 22–52 years). The healthy children were referred to the outpatient clinic of Necker-Enfants Malades Hospital, Paris, France, for diagnostic blood testing. The immunodeficiency cohort analyzed by using FACS consisted of 92 pediatric and adult patients assessed for follow-up or screening for a PID or CVID. The AT cohort analyzed by using PROMIDIS $\alpha$  consisted of 37 patients followed at the Necker Hospital. The genetic status of VDJ recombination-deficient (VDJ) patients and patients with AT enrolled in the PROMIDIS $\alpha$  analysis is presented in Table E1 in this article's Online Repository at [www.jacionline.org](http://www.jacionline.org). Peripheral venous blood samples were collected into EDTA and processed within 24 hours. All genetic studies were performed after retrieving written consent from the patient or for minors from their legal guardian. The study was performed in accordance with the modified version of the Helsinki Declaration.

### Whole TCR $\alpha$ repertoire determination using switching mechanism at the 5'-end of the RNA transcript (SMART)

Determination of a comprehensive TCR $\alpha$  repertoire by means of 5' rapid amplification of cDNA ends PCR/NGS (switching mechanism at the 5'-end of the RNA transcript [SMART]) was performed on peripheral blood lymphocytes (PBLs) from DNA ligase IV<sup>12</sup> and *Cernunnos*-deficient<sup>13</sup> patients by using Clontech's SMART technology (Clontech, Mountain View, Calif),<sup>14</sup> as previously described.<sup>11</sup> Sequencing on the Personal Genome Machine (PGM; IonTorrent, Life Technologies, South San Francisco, Calif) was performed according to the manufacturer's recommendations. Sequencing data were analyzed with LymAnalyzer<sup>15</sup> to retrieve unique complementarity-determining region 3 clonotypes and to determine T-cell receptor  $\alpha$  variable gene (TRAV) and T-cell receptor  $\alpha$  joining gene (TRAJ) segments. Output

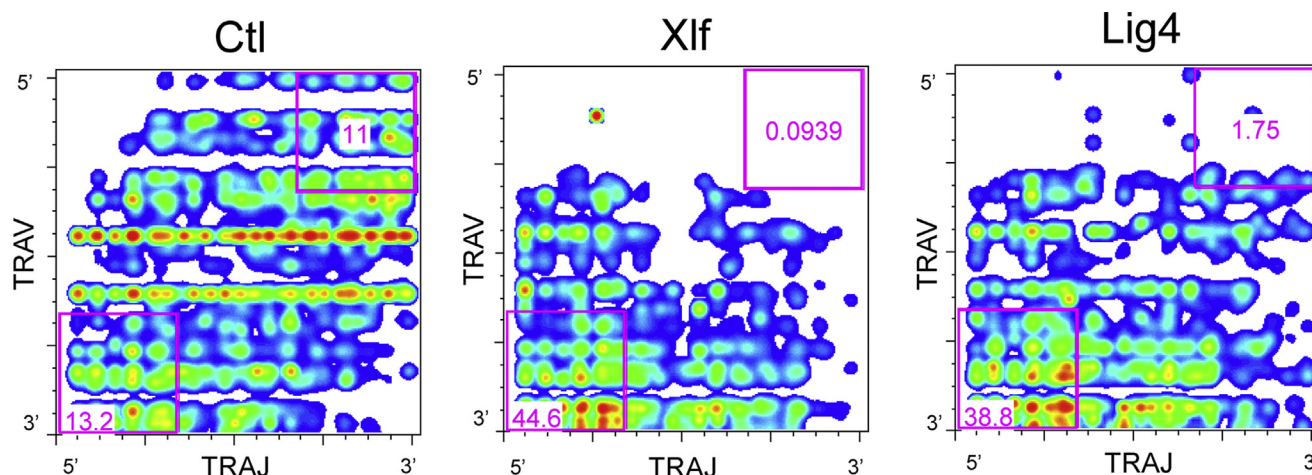


**FIG 1.** Comprehensive TCR $\alpha$  repertoire study. Two-dimensional heat map representation of TCR $\alpha$  transcripts determined by using 5' rapid amplification of cDNA ends (5' RACE)-PCR/NGS (SMART $\alpha$ ) according to TRAJ (*x*-axis) and TRAV (*y*-axis) elements. Lower left and upper right quadrants represent proximal (TRAV22-41/TRAJ61-J48) and distal (TRAV1-11/TRAJ17-1) TRAV/TRAJ associations, respectively. Clinical/genetic status, but not TCR $\alpha$  repertoire, were previously described for the Cernunnos/XLF<sup>13</sup> and Lig4<sup>12</sup> patients, respectively.

LymAnalyzer files were transformed with R software to generate FlowJo9 compatible files with genomic coordinates of the various TRAV and TRAJ pairs. TRAV and TRAJ use was determined by using FlowJo software (TreeStar, Ashland, Ore; Fig 1).<sup>12,13</sup> Gates were applied to score transcripts by using either proximal (TRAV22-41/TRAJ61-J48) or distal (TRAV1-11/TRAJ17-1) TRAVJ combinations.

## TRAV1 (V $\alpha$ 7.2) determination by using flow cytometry

For screening with FACS, 100  $\mu$ L of whole blood was incubated for 30 minutes at 4°C with 5  $\mu$ L of both indicated fluorochrome-labeled mAbs: allophycocyanin anti-CD3 (HIT3a; Sony, Weybridge, United Kingdom) and phycoerythrin anti-TCR V $\alpha$ 7.2 (3C10; Sony). After red cell lysis (FACS Lysing Solution; BD, Franklin Lakes, NJ) and washing of the remaining cells twice with cell wash buffer (BD), cells were fixed in a cell fixation solution (BD). CD3<sup>+</sup> cells were analyzed by means of flow cytometry within 24 hours (FACSCanto II; BD). Expression of TCR V $\alpha$ 7.2 on CD3<sup>+</sup> lymphocytes was assessed by using FlowJo software (Tree Star).

## Sampling of TCR $\alpha$ repertoire by using PROMIDIS $\alpha$

cDNA from PBLs was amplified with a series of 8 primers specific for Hu-TRAV segments representing proximal (TRAV35 and TRAV41), middle (TRAV20, TRAV21, and TRAV23), and distal (TRAV1, TRAV5, and TRAV10) TRAV segments together with TRAC3-REPF, a C $\alpha$ -specific primer.<sup>16</sup> Primers include an anchor sequence (RepF and RepR) for subsequent NGS sequencing on the PGM. PCR bands were gel purified and reamplified with PGM sequencing primers A\_BCx\_REP\_F 5'-CCATCTCATCCTGCGTGTCTCCGACTCAG XXXXXXXXXXXCGCCCATTTGACGCAAA-3', where xxx represent the barcode (BCx) sequence and P1\_REP\_R 5'-CCCTCTCTATGGGACGTCGGTG ATCCCTCGCCGGACACGCTGAA-3'; TRAV1-RepR, ccctcgccggacacgctgaa AGGTCGTTTTTCTTCTATCTCTAGTC; TRAV5-RepR, ccctcgccggacacgctg aaAAACAAGACCAAGACTCACTGTTCT; TRAV10-RepR, ccctcgccggacac cgtgaaTACAGCAACTCTGGATGCAGACAC; TRAV20-RepR, ccctcgccgga cagctgaaGCCACATTAACAAAGAAAGGAAAGCT; TRAV21-RepR, ccctc gccggacacgctgaaGCCTCGCTGGATAAATCATCAGGA; TRAV23-RepR, ccct cgccggacacgctgaaCAACATCTCCTTCAATAAAAGTGCCA; TRAV35-Rep, c cctcgccggacacgctgaaCTCAGTTTGGTATAACCAGAAAGGA; TRAV41-RepR, ccctcgccggacacgctgaaGATTAATTGCCACAATAAACATACAGG; and TRAC3-RepF, cgcccatgacgcaaaGTCAGTGGATTAGAGTCTCTCAG.

Sequencing on the PGM was performed according to the manufacturer's recommendations, metrics of which are presented in Fig E1 in this article's Online Repository at [www.jacionline.org](http://www.jacionline.org). Raw sequencing data were analyzed as for SMART $\alpha$ . TRAV and TRAJ use was quantified by using FlowJo software. Nine parameters were extracted: frequencies of Vprox (TRAV35 and TRAV41), Vmid (TRAV20, TRAV21, and TRAV23), and Vdist (TRAV1, TRAV5, and TRAV10) and frequencies of Jprox (TRAJ61-48) and Jdist (TRAJ17-1) within each TRAV category. Principal component analysis (PCA) and hierarchical clustering were performed on these 9 parameters by using the PCA() and HCPC() functions of the FactoMineR package, respectively (<http://factominer.free.fr/>),<sup>17</sup> and graphics were generated with the Factoextra R package (<http://www.sthda.com/english/rpks/factoextra>).<sup>18</sup> Statistical analyses covering the 9 parameters were performed by using the Hotelling T<sup>2</sup> test (Real Statistics Resource Pack for Excel, release 4.3; copyright [2013–2015] Charles Zaiontz, [www.real-statistics.com](http://www.real-statistics.com)). One-parameter representations were performed with Prism 6 software (GraphPad Software, La Jolla, Calif), with Statistical analysis performed by using the Mann-Whitney nonparametric *t* test.

## RESULTS

### TCR $\alpha$ repertoire bias in DNA repair-deficient patients

One singularity of the TCR $\alpha$  locus over the other TCR and immunoglobulin genes consists of its multiple-wave somatic rearrangement process. It initiates with the particular TCR $\delta$  recombination element/ $\Psi$ J $\alpha$  recombination event, which associates the noncoding TCR $\delta$  recombination element (T-cell receptor  $\delta$  recombination element) upstream of the TCR $\delta$  locus with the most 5' J $\alpha$  segment (TRAJ61 or  $\Psi$ J $\alpha$ ).<sup>19</sup> Subsequent waves of recombination associate more upstream TRAV segments to more downstream TRAJ elements until thymocyte-positive selection arrests the process by downregulating RAG1/2 expression.<sup>20</sup>

This mechanism has 2 practical implications. First, a correlation exists between TRAV and TRAJ elements present in TCR $\alpha$  transcripts (ie, proximal 3' TRAV elements being preferentially associated with proximal 5' TRAJs and conversely distal 5' TRAVs with distal 3' TRAJs).<sup>21</sup> Second, TCR $\alpha$



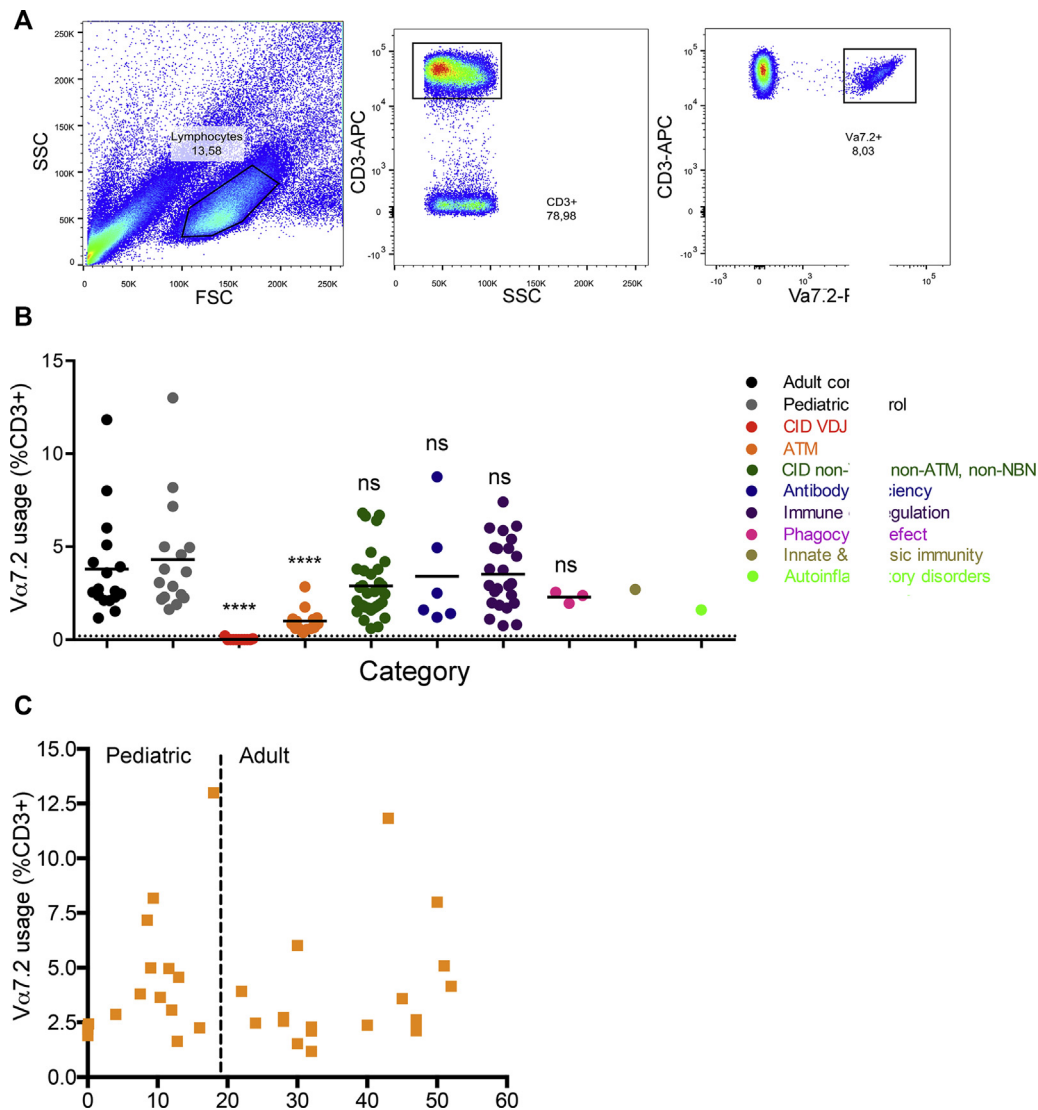


**FIG 2.** Analysis of TCR-V $\alpha$ 7.2-expressing T lymphocytes by using FACS. **A**, Gating strategy to quantify TCR-V $\alpha$ 7.2 (V $\alpha$ 7.2-phycoerythrin)-expressing T lymphocytes among CD3<sup>+</sup> T cells (CD3-allophycocyanin [APC]) in whole blood. **B**, Frequencies of V $\alpha$ 7.2-positive T cells in 92 patients with PIDs of various cause, 17 adult healthy control subjects, and 16 pediatric (<18 years) healthy control subjects. **C**, Representation of V $\alpha$ 7.2 T-cell frequency in healthy control subjects according to age. The limit between adult and pediatric is set at 18 years of age. \*\*\*\* $P$  < .0001, Mann-Whitney statistical test. ns, Not significant.

repertoire diversity is linked to the thymocyte lifespan. The TCR $\alpha$  repertoire is biased toward use of more distal 5' TRAVs/3' TRAJs when the thymocyte lifespan is increased artificially by expression of a Bcl-x(L) transgene.<sup>22</sup> Conversely, reducing thymocyte lifespan (eg, in RAR-related orphan receptor  $\gamma$ T [ROR $\gamma$ T] KO mice<sup>23</sup>) results in a TCR $\alpha$  repertoire biased toward more proximal 3' TRAV/5' TRAJ associations.

Previously, we noticed that T lymphocytes from *Xlf* KO mice displayed a biased TCR $\alpha$  repertoire toward proximal TRAV/-TRAJ recombination events, which is consistent with the reduced viability of their thymocytes, as judged by their increased *ex vivo* apoptosis.<sup>11</sup> We extended this observation in human subjects by analyzing characteristics of T cells from 2 immunodeficient patients with Cernunnos/*XLFI* and DNA ligase IV mutations, respectively. As shown in Fig 1, the whole TCR $\alpha$  repertoire analyzed by using SMART $\alpha$  was biased in these 2 patients because TCR $\alpha$  transcripts associating proximal TRAV

and TRAJ elements (lower left quadrant) accounted for 44.6% and 38.8%, respectively, compared with 13.2% in healthy control subjects. Conversely, TCR $\alpha$  transcripts with distal TRAVs/TRAJs (upper right quadrant) were barely detectable in these 2 patients (0.09% and 1.75%, respectively, compared with 11% in the healthy control subjects). In light of these observations, we considered that analyzing the TCR $\alpha$  repertoire could indeed represent a valuable biomarker to assist in diagnosis of the various pathologies affecting the development of the immune system.

### Diagnosis of hypomorphic V(D)J recombination deficiencies through TCR-V $\alpha$ 7.2 determination by using FACS

The easiest way to analyze the TCR $\alpha$  repertoire on a large series of patients would be to score TRAV expression by using FACS. Unfortunately, very few anti-TRAV-specific antibodies

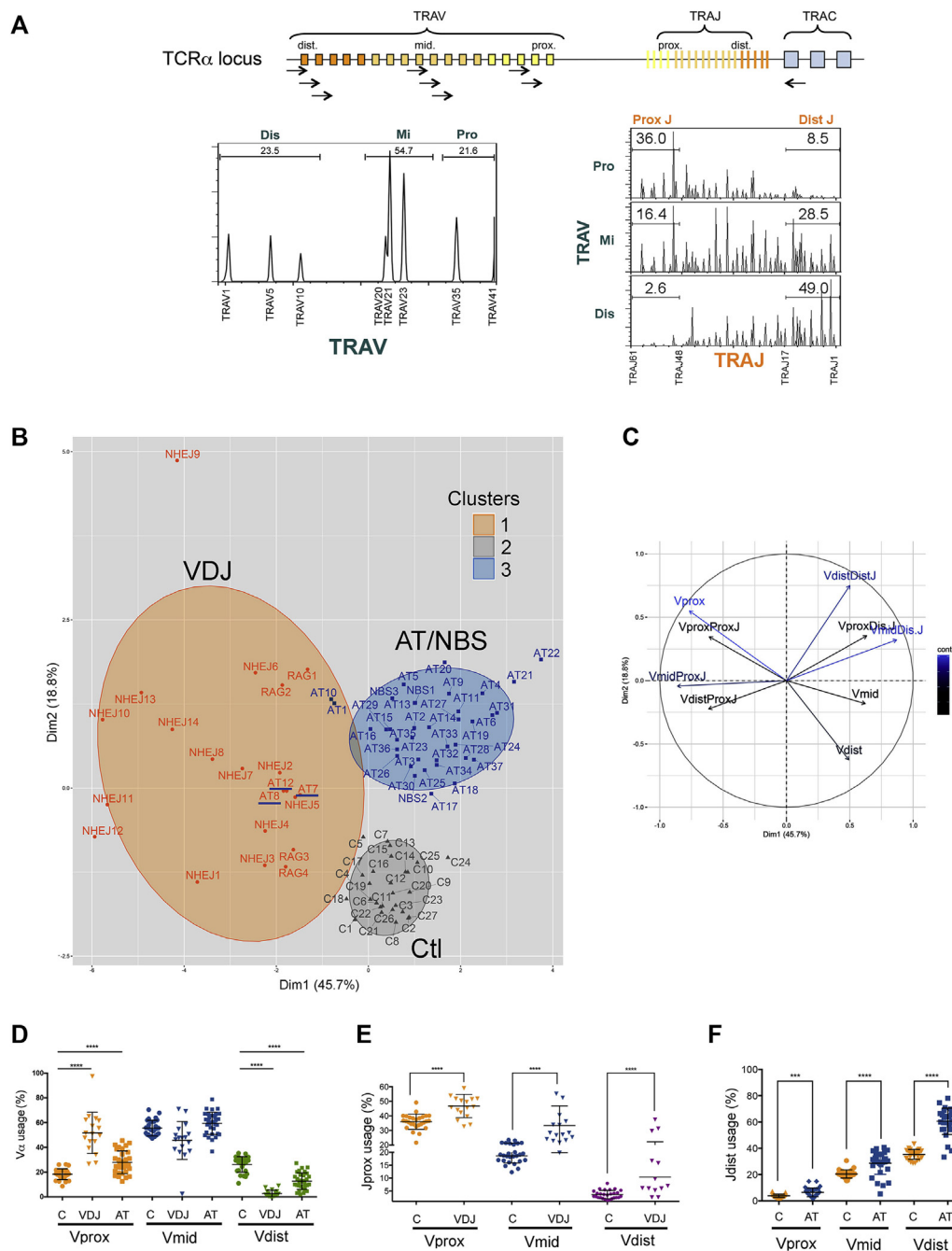


**FIG 3.** TCR $\alpha$  repertoire analysis by using PROMIDIS $\alpha$ . **A**, TCR $\alpha$  loci and primers used for PCR amplification. TRAV use and TRAJ frequencies among proximal, medium, and distal TRAVs in unique TCR $\alpha$  clonotypes. Proximal TRAJ segments include TRAJ1 to TRAJ48, and distal TRAJ segments include TRAJ17 to TRAJ1. **B**, Unsupervised hierarchical clustering of 85 tested subjects (27 control subjects, 18 VDJ patients, 37 patients with AT, and 3 patients with NBS). VDJ patients are labeled *NHEJ* or *RAG* depending on their gene defect, as shown in Table E1. The 3 patients with AT who cluster with VDJ patients are underlined in blue. **C**, Contributions of the variables underlying the PCA and hierarchical clustering analysis from dark blue (weak contribution) to light blue (high contribution). **D**, Single-parameter analysis of TRAV use between control subjects (circles), V(D)J patients (triangles), and patients with AT (squares) for each TRAV subgroup. **E**, Proximal TRAJ use between control subjects (circles) and V(D)J patients (triangles) for each TRAV subgroup. **F**, Distal TRAJ use in control subjects (circles) and patients with AT (squares). \*\*\* $P < .001$  and \*\*\*\* $P < .0001$ , Mann-Whitney nonparametric  $t$  test.

**TABLE I.** V(D)J recombination–defective patients identified by absent V $\alpha$ 7.2-positive T cells

	P1/VDJ8	P2/VDJ18	P3/VDJ7*	P4†	P5/VDJ17
Sex	F	M	F	M	F
Molecular diagnosis‡	P	R	R	R	P
Age at diagnosis (y)	28	9	9	15	34
Clinical phenotype	CID	CID	CID-G/AI	CID-G/AI	CID-G/AI
Infections	LRTI with bronchiectasis Invasive aspergillosis HPV infection	LRTI with bronchiectasis Extended varicella	LRTI	LRTI with bronchiectasis	Regional BCG-itis URTI and LRTI
Autoimmunity			Autoimmune myasthenia Alopecia, vitiligo	Cytopenia (ITP, neutropenia)	Autoimmune epidermolysis bullosa, vitiligo, premature ovarian failure, hypothyroidism
Other manifestations	EBV-associated leiomyosarcoma			Systemic granulomatosis caused by rubella vaccine strain	Asthma
Mutations	<i>DCLRE1C</i> p.D20H p.T167M	<i>DCLRE1C</i> c.1290-1306del/ c.1290-1306delb/	<i>RAG1</i> p.H375D/p.R410W	<i>RAG1</i> p.H375D/p.Y562C	<i>RAG1</i> p.R474C/p.R918-F919delinsL
Immunophenotyping					
CD3 <sup>+</sup> (number/mm <sup>3</sup> )	601 (807-1844)	176 (1200-2600)	273 (1200-2600)	469 (1000-2200)	2125 (807-1844)
V $\alpha$ 7.2/CD3 <sup>+</sup> (%)	0.2	0	0	0	0
T CD4 <sup>+</sup> cells (number/mm <sup>3</sup> )	313 (460-1232)	126 (650-1500)	169 (650-1500)	418 (530-1300)	925 (460-1232)
T CD8 <sup>+</sup> cells (number/mm <sup>3</sup> )	288 (187-844)	42 (370-1100)	42 (370-1100)	20 (330-920)	875 (187-844)
CD45RA <sup>+</sup> CD31 <sup>+</sup> /CD4 (%)	ND	1 (43-55)	3 (43-55)	ND	3 (30-48)
CCR7 <sup>+</sup> CD45RA <sup>+</sup> /CD8 (%)	ND	4 (52-68)	19 (52-68)	ND	8 (37-50)
$\gamma\delta$ /CD3 <sup>+</sup> (%)	ND	5	24	3	18
B cells (number/mm <sup>3</sup> )	5 (92-420)	4 (219-509)	56 (270-860)	20 (193-628)	150 (169-271)
NK cells (number/mm <sup>3</sup> )	564 (89-362)	160 (100-480)	150 (100-480)	20 (70-480)	200 (89-362)

AHAI, Autoimmune hemolytic anemia; CID-G/AI, combined immunodeficiency with granuloma or autoimmunity; F, female; HPV, human papilloma virus; ITP, idiopathic thrombocytopenic purpura; LRTI, low respiratory tract infection; M, male; ND, not determined; URTI, upper respiratory tract infection.

\*Reported as P4 in Rowe et al.<sup>24</sup>

†Reported as patient 5 in Neven et al.<sup>25</sup>

‡Molecular diagnosis: prospective (P) or retrospective (R).

§P9 is the brother of a previously identified patient with CID with a *PRKDC* mutation.

are available, and none are available to track proximal TRAV use. Nevertheless, one antibody, 3C10, is directed toward TCR-V $\alpha$ 7.2, a TRAV segment expressed by human mucosal-associated invariant T lymphocytes<sup>23</sup> that represents the most distal (upstream) TCR $\alpha$  segment, TRAV1. We used this antibody to analyze 92 blood samples from patients assessed for screening or follow-up of immunodeficiencies by using FACS, excluding cases of “classical” T<sup>+</sup>B<sup>+</sup>NK<sup>+</sup> SCID (Fig 2, B). This series included 11 patients with PIDs related to V(D)J recombination deficiency (red category in Fig 2, B, and Table I),<sup>24,25</sup> 14 patients with AT (orange category in Fig 2, B), and 67 patients with a various spectrum of PIDs. The frequency of TCR-V $\alpha$ 7.2–expressing CD3<sup>+</sup> T lymphocytes was highly heterogeneous, with means ranging from 0.02% to 3.5%. Among the various categories of immunodeficiencies, only patients with combined immunodeficiency (CID) with V(D)J recombination defects (CID-VDJ) and the patients with AT had a frequency of V $\alpha$ 7.2–expressing T cells that were statistically reduced (0.02% and 1.00%, respectively;  $P < .0001$ ) compared with those in pediatric control subjects (Fig 2, B, gray dots; 4.31%). The frequency of TCR-V $\alpha$ 7.2–expressing T cells did not vary with age (Fig 2, C) because the difference between mean values of pediatric and adult healthy control subjects was not significant ( $4.31\% \pm 2.98\%$  and  $3.80\% \pm 2.70\%$ , respectively;  $P = .57$ ).

The 11 patients with CID-VDJ (red category in Fig 2, B) were almost completely devoid of TCR-V $\alpha$ 7.2–expressing T cells

(mean, 0.02%), a situation never encountered in control subjects or in other tested patients. These patients ranged from newborn to 34 years of age and presented with combined CIDs mostly characterized by decreased numbers of both T and B lymphocytes often associated with a sharp decrease in CD45RA<sup>+</sup>CD31<sup>+</sup>/CD4<sup>+</sup> and CD8<sup>+</sup> naive T cells (Table I). These 11 patients harbored deleterious biallelic mutations in genes involved in the V(D)J recombination (*RAG1* [n = 8], DNA cross-link repair 1C/Artemis [*DCLRE1C*; n = 2], and protein kinase, DNA-activated, catalytic polypeptide [*PRKDC*; n = 1]). For 5 of them, the molecular defect was known before V $\alpha$ 7.2 analysis (R), whereas for the remaining 6, the absence of V–7.2–expressing T cells oriented the sequencing effort toward the V(D)J recombination candidate genes in a prospective manner (P). Importantly, apart from these 11 cases, none of the other 81 patients carried mutations in any of the classical V(D)J recombination–associated genes. Thus this first series of analyses demonstrated the usefulness of examining part of the TCR $\alpha$  repertoire as a tool to help in the diagnosis of hypomorphic V(D)J recombination deficiencies.

We next extended this V $\alpha$ 7.2 FACS survey to a group of 14 patients with AT given the known implication of the DNA repair factor ATM to both cell survival and V(D)J recombination.<sup>26</sup> The frequency of V $\alpha$ 7.2–expressing T cells was reduced severely in the AT group ( $1.00\% \pm 0.63\%$  compared with  $4.31\% \pm 2.98\%$  in pediatric control subjects; orange category in Fig 2, B),

TABLE I. (Continued).

P6	P7/VDJ9	P8	P9	P10	P11/VDJ10
F	M	M	M	M	M
P	R	P	P	P	R
2	8	7	1	0.2	1
CID	CID-G/AI	CID with AIHA	CID	Omenn syndrome	§
Respiratory tract infections	URTI and	URTI and	Disseminated infection		
Recurrent diarrhea	LRTI with bronchiectasis	LRTI with bronchiectasis	to adenovirus		
EBV and CMV replication	Molluscum contagiosum				
	AHAI	AHAI			
	Hepatopathy				
	Chronic enteropathy				
<i>RAG1</i>	<i>RAG1</i>	<i>RAG1</i>	<i>RAG1</i>	<i>RAG1</i>	<i>PRKDC</i>
p.H612R/p.H612R	p.G816R/p.G816R	p.E174SfsX27/p.P619L	p.R474H/p.R559S	c.519delT/c.519delT	p.L3062R/ p.L3062R
2248 (2100-6200)	1423 (1200-2600)	1004 (1200-2600)	1372 (2100-6200)	6297 (2500-5500)	ND
0	0	0	0	0	0
519 (1300-3400)	388 (650-1500)	414 (650-1500)	457 (1300-3400)	5634 (1600-400)	ND
303 (620-2000)	808 (370-1100)	430 (370-1100)	600 (620-2000)	663 (560-1700)	ND
2 (57-65)	1 (43-55)	2 (43-55)	5 (57-65)	0.2 (60-72)	ND
2 (52-68)	0.5 (52-68)	7 (52-68)	0.5 (52-68)	0.2 (52-68)	ND
61	30	ND	22	1	ND
1211 (319-1244)	2 (219-509)	143 (273-860)	114 (523-2149)	3 (712-2059)	ND
130 (180-920)	49 (100-480)	383 (100-480)	1200 (180-920)	265 (170-1100)	ND

a decrease that was highly statistically significant ( $P < .0001$ ). However, although the V $\alpha$ 7.2 frequency is clearly informative at the population level, it cannot be satisfactorily used to assist in diagnosis at the individual level given the overlap between V $\alpha$ 7.2 values observed in patients with AT and control subjects. Several studies have shown that mucosal-associated invariant T lymphocytes, which can be distinguished from conventional TCR-V $\alpha$ 7.2-positive T cells by their specific expression of the cell-surface marker CD161, account for the vast majority of total V $\alpha$ 7.2-positive T cells in peripheral blood of healthy subjects.<sup>27-29</sup> However, their frequency fluctuates greatly and is severely reduced in various conditions of immune deregulation, such as HIV infection or severe bacterial infections.<sup>27-29</sup> As a consequence, the total number of V $\alpha$ 7.2-expressing lymphocytes decreases considerably in these situations. This might contribute to the wide distribution in the frequency of V $\alpha$ 7.2-positive T cells we observed in the 125 analyzed subjects presented in Fig 2. Therefore the sole scoring of V $\alpha$ 7.2-positive T cells cannot be used reliably to assist in the diagnosis of most patients with AT. This prompted us to develop a more robust resource for analyzing possible bias in TCR $\alpha$  use.

### PROMIDIS $\alpha$ : A TCR $\alpha$ repertoire signature to identify PIDs

SMART $\alpha$  and FACS analysis (Fig 2) paved the way to using TCR $\alpha$  repertoire determination as an attractive tool to assist in

the diagnosis of PIDs. Yet neither of these experimental approaches can be envisioned as a biomarker for individual diagnostic purposes. SMART $\alpha$  allows the most comprehensive TCR $\alpha$  repertoire analysis but is technically very challenging for most routine laboratory work. On the other hand, FACS analysis with anti-V $\alpha$ 7.2 antibody is simple and cost-effective but is not robust enough in many instances, as discussed above.

To combine robustness and simplicity, we analyzed the relative use frequency of 8 different TRAV genes (and their associated TRAJ element) dispersed on the locus as proximal, middle, and distal elements, hence the PROMIDIS $\alpha$  denomination, by using RT-PCR and NGS in a multiplex PCR (Fig 3, A). After RT-PCR/NGS, unique clonotypes expressed by TCR $\alpha$  transcripts were identified and scored with LymAnalyzer<sup>15</sup> from raw sequencing files. We then calculated relative proportions of proximal (TRAV35 and TRAV41), middle (TRAV20, TRAV21, and TRAV23), and distal (TRAV1, TRAV5, and TRAV10) TCR $\alpha$  transcripts and the frequency of proximal (TRAJ61-TRAJ48) and distal TRAJ (TRAJ17-TRAJ1) elements within each of these subgroups, for a total of 9 parameters. As shown in Fig 3, A, this analysis faithfully reflected the TCR $\alpha$  peculiarity of TRAV/TRAJ correlation.<sup>21</sup> Indeed, TCR $\alpha$  transcripts containing proximal TRAVs were associated predominantly with proximal TRAJs (36%) as opposed to distal ones (8.5%). Conversely, TCR $\alpha$  transcripts using distal TRAVs were predominantly associated with distal TRAJs (49%) as opposed to proximal ones (2.6%).

We next incorporated the values of these 9 parameters in PCA and hierarchical clustering analyses to survey 27 healthy control subjects, 18 patients with PIDs with mutations in components of the V(D)J recombination machinery (*RAG1* [n = 4], *DCLRE1C/Artemis* [n = 5], *PRKDC/DNAKcs* [n = 2], DNA ligase IV [n = 3], and Cernunnos/*XLFI* [n = 4]), 37 patients with AT, and 3 patients with NBS. Genotypes of the patients are recorded in Table E1. Six of the VDJ patients had their V $\alpha$ 7.2-expressing T cells scored by using FACS (Fig 2 and Table I). Unsupervised hierarchical clustering analysis (Fig 3, B) revealed partitioning of these 85 subjects into 3 groups, one comprising the 27 control subjects, one comprising the 18 VDJ patients, and one comprising the majority of the patients with AT and the 3 patients with NBS. Of note, none of the VDJ patients or patients with AT/NBS were assigned to the control group, and conversely, none of the 27 control subjects clustered with either the VDJ patients or the patients with AT/NBS. A slight overlap between the VDJ patients and the patients with AT/NBS was noticed for 3 patients with AT (AT7, AT8, and AT12) clustering within the VDJ group. The clustering was highly statistically significant between the VDJ patients and control subjects ( $P = 3.30E-16$ , Hotelling  $T^2$  test), as well as between the patients with AT/NBS and the VDJ patients ( $P = 1.28E-07$ , Hotelling  $T^2$  test). Consideration of the 9 variables contributing to PCA (Fig 3, C) was clearly indicative of a bias in TCR $\alpha$  use toward proximal TRAVs and TRAJs in VDJ patients. One-parameter analysis (Fig 3, D and E) of the various variables demonstrated that TRAV/TRAJ use in T cells from VDJ patients was severely skewed toward the use of more proximal TRAV elements (mostly to the expense of distal ones), with statistically significant differences in the 3 classes of TRAVs between control subjects and patients (Fig 3, D).

In addition, when considering TRAJ use (Fig 3, E), the repertoire of VDJ patients was biased toward use of proximal TRAJs within the 3 classes of TRAVs. This was particularly striking within the few TCR $\alpha$  transcripts using distal TRAV elements, in which proximal TRAJ elements are usually largely underrepresented in T cells from control subjects. These observations outlined a specific TCR $\alpha$  repertoire signature in VDJ patients, which recapitulates the bias identified by using SMART $\alpha$  (ie, a sharp decrease in distal TRAV/TRAJ use within TCR $\alpha$  transcripts associated with an increase in more proximal TRAV and TRAJ elements). The PROMIDIS $\alpha$  signature is consistent with reduced V(D)J recombination efficacy in thymocytes from these patients but could also reflect decreased thymocyte viability in patients harboring mutations in DNA repair encoding genes, as previously observed in *Xlf* KO mice.<sup>11</sup> Therefore the PROMIDIS $\alpha$  signature in mature peripheral T lymphocytes represents a reliable marker of the V(D)J recombination activity/thymocyte lifespan during thymocytes development. This signature is very specific because none of 44 analyzed patients with non-VDJ-associated PIDs clustered in the VDJ group (see Fig E1).

### Early identification of patients with AT through a specific PROMIDIS $\alpha$ signature

PROMIDIS $\alpha$  was used to analyze the TCR $\alpha$  repertoire in a series of 37 patients with AT and 3 patients with NBS, 6 in a prospective manner based on the sole clinical presentation and before knowledge of the underlying ATM mutations, to extend the observation of a bias, as suggested by FACS analysis with

V $\alpha$ 7.2 staining in PBLs (Fig 2). As shown in Fig 3, B, most of the patients with AT/NBS clustered in a separate group from the VDJ patients ( $P = 1.28E-07$ , Hotelling  $T^2$  test) and control subjects. Three patients (AT7, AT8, and AT12) clustered within the VDJ subgroup. The survey of more cases is now required to assess whether this misclustering reflects a meaningful structure/function relationship of the underlying mutations. The contributions of individual variables in the PCA (Fig 3, C) suggested that TCR $\alpha$  transcripts from patients with AT and NBS were skewed toward the proximal TRAV use also seen in the signature of VDJ patients. However, in sharp contrast to VDJ patients, the TCR $\alpha$  transcripts from patients with AT and NBS were biased toward use of distal TRAJ elements, as opposed to expected proximal TRAJs. One-parameter analysis confirmed both the increase in proximal TRAV use (Fig 3, D) at the expense of distal TRAVs and the increase in distal TRAJ association in all TRAV subgroups (Fig 3, F). The same bias toward use of distal TRAJ elements was also observed in T lymphocytes and thymocytes from *Atm* KO mice (data not shown). The exact molecular mechanism causing the TRAJ bias specifically observed in patients with *ATM* and *NBN* deficiencies is not presently understood. In any case, the striking difference between PROMIDIS $\alpha$  signatures of patients with AT/NBS and VDJ patients provides a specific marker that helps identify patients with AT/NBS.

### DISCUSSION

Here we describe the development of a new immunologic biomarker based on analysis of the TCR $\alpha$  repertoire designed to assist the diagnosis of patients with PIDs characterized by hypomorphic defects in the V(D)J recombination process, alteration of the DNA damage response, or both. Although most TCR and immunoglobulin gene rearrangements proceed through a unique wave of somatic recombination, the TCR $\alpha$  locus adopts a directional multistep recombination process that is arrested by downregulation of *RAG1/2* expression on positive selection of thymocytes expressing sound TCR specificity on their surfaces.<sup>20</sup> As a consequence, although slightly reduced V(D)J recombination efficacy might have no visible detrimental effect on most TCR and immunoglobulin loci, the persistent reduced recombinase activity over successive waves of TCR $\alpha$  rearrangement translates to a bias in TCR $\alpha$  use, as described here.

FACS analysis can readily highlight this bias through sole quantification of TCR-V $\alpha$ 7.2-expressing T lymphocytes when V(D)J activity decreases to less than a certain threshold, as shown in a series of 11 patients. It can be more precisely characterized by analyzing 9 parameters related to the various types of TRAV and TRAJ gene use among TCR $\alpha$  transcripts through PROMIDIS $\alpha$ , a multiplex RT-PCR followed by deep sequencing, as shown here for 18 patients with PIDs with variable V(D)J recombination deficiency and patients with 37 AT/NBS.

Human conditions with mutations in either *RAG1* or *RAG2* genes constitute the prototypical example of the broad spectrum of clinical consequences that patients can present depending on their specific *RAG1/2* gene mutation and hence the residual activity of the V(D)J recombination during T- and B-cell maturation.<sup>5-7</sup> At one end of the spectrum, complete *RAG1/2* loss of function leads to classical T<sup>-</sup>B<sup>-</sup> SCID. On the other end, depending on the hypomorphic status of their mutations, patients can present with various degrees of immune dysfunction



up to mild autoimmunity. In particular, PROMIDIS $\alpha$  can help identify cases of late-onset immunodeficiency, as presented by both adult patients (P1 and P5) included in our series.

Overall, the near absence of V $\alpha$ 7.2-expressing T cells together with the VDJ-specific PROMIDIS $\alpha$  signature in 6 cases prospectively oriented the molecular study to direct Sanger DNA sequencing of VDJ recombination candidate genes, with identification of underlying mutations in all cases rather than sequencing with a PID-specific gene panel or whole-exome sequencing, which accelerated considerably the diagnosis and decreased its cost. These 2 combined assays are very robust and of high predictive value for PIDs with hypomorphic V(D)J recombination deficiency because no mutations in V(D)J recombination candidate genes could be found in the 92 TCR-V $\alpha$ 7.2-analyzed patients outside the 11 identified with almost complete absence of V $\alpha$ 7.2-expressing T cells. Likewise, all 18 patients with mutations in V(D)J recombination-related genes and none of the 27 control subjects or 44 patients with PIDs with non-VDJ presentation displayed specific VDJ or AT/NBS PROMIDIS $\alpha$  signatures. PROMIDIS $\alpha$  should be very valuable also for the retrospective *in vivo* functional validation of variants identified through whole-exome sequencing. With respect to *RAG1/2* mutations, extensive studies from the Notarangelo laboratory have linked the clinical status of VDJ-defective patients to the residual level of recombinase activity tested through *in vitro* complementation of defective vAbl transformed pro-B-cell lines by using retroviral expression of exogenous *RAG1/2* mutants (for review see Notarangelo et al<sup>5</sup>). In some cases results of these complementation studies do not concord with the observed clinical condition, and thus PROMIDIS $\alpha$  might represent an interesting alternative for *in vivo* validation of the identified variants.

In contrast to control subjects, the distribution of TCR-V $\alpha$ 7.2-positive T lymphocytes in patients with PIDs is highly heterogeneous. Thus more systematic studies using PROMIDIS $\alpha$  are required to provide an in-depth characterization of changes in TRAV and TRAJ use characteristics and their possible defects in various PIDs. It is known that, in addition to (or together with in some cases) the V(D)J recombination machinery *per se*, alterations of the thymocyte lifespan can exert a major effect on TCR $\alpha$  repertoire generation. Mice with a targeted inactivation of the ROR $\gamma$ T transcription factor are characterized by thymocytes with a reduced lifespan, which translates into a bias in V $\alpha$ J $\alpha$  use toward the most proximal gene segments.<sup>22</sup> Likewise, T cells from patients with mutations in the RAR-related orphan receptor C (*RORC*) gene encoding the human ROR $\gamma$ T counterpart exhibit a similar bias,<sup>30</sup> which can be recapitulated by *in silico* PROMIDIS $\alpha$  (data not shown). Therefore one can hypothesize that mutations in genes that encode factors involved in distinct aspects of thymocyte development could affect the TCR $\alpha$  repertoire, which can then be revealed in peripheral mature T lymphocytes by using PROMIDIS $\alpha$ . Of note, study of the TCR $\alpha$  repertoire bias we describe here is an echo of a very specific window of T-cell maturation in the thymus (ie, the CD4/CD8 double-positive stage, during which essentially noncycling thymocytes undergo TCR $\alpha$  rearrangement). It does not apply to upstream maturation events, such as TCR $\beta$  rearrangements and  $\beta$ -selection, or downstream steps, such as transition to CD4 and CD8 single-positive mature thymocytes or egress from the thymus or any event in the periphery. In that respect one could hypothesize that conditions

with impaired positive selection can translate into a specific bias in TCR $\alpha$  use, but our preliminary experiments using MHC class I and II KO mice do not sustain this hypothesis (unpublished observations). Analyzing patients with HLA deficiency should be interesting in that regard.

In this study we also established that PROMIDIS $\alpha$  constitutes a particularly valuable biomarker to help identify patients with AT and those with NBS because we showed that mutations in the *ATM/NBN* genes result in a very specific TCR $\alpha$  signature. This should help in the care of patients with AT/NBN, particularly in prevention of acute infections and the possibility of prenatal diagnosis in selected families. Likewise, PROMIDIS $\alpha$  could be of interest for the further investigation of patients with T-cell lymphopenia identified through newborn screening.<sup>31</sup> Finally, whether the altered signature identified in patients with AT/NBS and patients with mutations in *Cernunnos/XLF*, DNA ligase IV, *DCLRE1C/Artemis*, and *PRKDC* can be found in other conditions of DNA repair deficiency will be of particular interest. Indeed, many of these patients are prone to cancer development for which treatments are often based on DNA damage-inducing drugs with a high risk of toxicity, as previously described in the first identified Lig4 patient, who succumbed after cranial radiotherapy as part of his antileukemia treatment.<sup>32,33</sup>

We thank all patients and their families for having agreed to participate in this study. We thank Stéphanie Ndaga, Aminata Diabate, Corinne Jacques, and Barick Konte for excellent technical assistance. We thank the Imagine Institute genomic platform for NGS sequencing and the French Institute of Bioinformatics (ANR-11-INBS-0013) for providing storage and computing resources on its national life science cloud.

#### Key messages

- Suboptimal V(D)J recombination activity results in bias in TCR $\alpha$  use.
- PROMIDIS $\alpha$  reveals specific TCR $\alpha$  signatures in patients with CID, AT, and NBS.
- PROMIDIS $\alpha$  might help identify patients with hypomorphic DNA repair deficiency.

#### REFERENCES

1. Tonegawa S. Somatic generation of antibody diversity. *Nature* 1983;302:575-81.
2. Schatz DG, Swanson PC. V(D)J recombination: mechanisms of initiation. *Annu Rev Genet* 2011;45:167-202.
3. Alt FW, Zhang Y, Meng FL, Guo C, Schwer B. Mechanisms of programmed DNA lesions and genomic instability in the immune system. *Cell* 2013;152:417-29.
4. de Villartay JP, Fischer A, Durandy A. The mechanisms of immune diversification and their disorders. *Nat Rev Immunol* 2003;3:962-72.
5. Notarangelo LD, Kim MS, Walter JE, Lee YN. Human RAG mutations: biochemistry and clinical implications. *Nat Rev Immunol* 2016;16:234-46.
6. Lee YN, Frugoni F, Dobbs K, Tirosh I, Du L, Ververs FA, et al. Characterization of T and B cell repertoire diversity in patients with RAG deficiency. *Sci Immunol* 2016;1.
7. Yu X, Almeida JR, Darko S, van der Burg M, DeRavin SS, Malech H, et al. Human syndromes of immunodeficiency and dysregulation are characterized by distinct defects in T-cell receptor repertoire development. *J Allergy Clin Immunol* 2014; 133:1109-15.
8. Gatti R, Perlman S. Ataxia-telangiectasia. In: Pagon RA, Adam MP, Ardinger HH, Wallace SE, Amemiya A, Bean LJH, editors. *Seattle: GeneReviews*; 1993.
9. Varon R, Vissinga C, Platzer M, Cerosaletti KM, Chrzanoska KH, Saar K, et al. Nibrin, a novel DNA double-strand break repair protein, is mutated in Nijmegen breakage syndrome. *Cell* 1998;93:467-76.

10. Schuetz C, Neven B, Dvorak CC, Leroy S, Ege MJ, Pannicke U, et al. SCID patients with ARTEMIS vs RAG deficiencies following HCT: increased risk of late toxicity in ARTEMIS-deficient SCID. *Blood* 2014;123:281-9.
11. Vera G, Rivera-Munoz P, Abramowski V, Malivert L, Lim A, Bole-Feysot C, et al. Cernunnos deficiency reduces thymocyte life span and alters the T cell repertoire in mice and humans. *Mol Cell Biol* 2013;33:701-11.
12. Dard R, Herve B, Leblanc T, de Villartay JP, Collopy L, Vulliamis T, et al. DNA ligase IV deficiency: Immunoglobulin class deficiency depends on the genotype. *Pediatr Allergy Immunol* 2017;28:298-303.
13. Cipe FE, Aydogmus C, Babayigit Hocaoglu A, Kilic M, Kaya GD, Yilmaz Gulec E. Cernunnos/XLF deficiency: a syndromic primary immunodeficiency. *Case Rep Pediatr* 2014;2014:614238.
14. Zhu YY, Machleder EM, Chenchik A, Li R, Siebert PD. Reverse transcriptase template switching: a SMART approach for full-length cDNA library construction. *Biotechniques* 2001;30:892-7.
15. Yu Y, Ceredig R, Seighe C. LymAnalyzer: a tool for comprehensive analysis of next generation sequencing data of T cell receptors and immunoglobulins. *Nucleic Acids Res* 2016;44:e31.
16. Han A, Glanville J, Hansmann L, Davis MM. Linking T-cell receptor sequence to functional phenotype at the single-cell level. *Nat Biotechnol* 2014;32:684-92.
17. Le S, Josse J, Husson F. FactoMineR: an R package for multivariate analysis. *J Stat Software* 2008;25:1-18.
18. Kassambara A. Practical guide to cluster analysis in R: STHDA. Available at: <http://sthda.com>. Accessed 2017.
19. de Villartay JP, Hockett RD, Coran D, Korsmeyer SJ, Cohen DI. Deletion of the human T-cell receptor  $\alpha$ -gene by a site-specific recombination. *Nature* 1988;335:170-4.
20. Brandle D, Muller C, Rulicke T, Hengartner H, Pircher H. Engagement of the T-cell receptor during positive selection in the thymus down-regulates RAG-1 expression. *Proc Natl Acad Sci U S A* 1992;89:9529-33.
21. Mauvieux L, Villey I, de Villartay JP. T early alpha (TEA) regulates initial TCRVJA rearrangements and leads to TCRJA coincidence. *Eur J Immunol* 2001;31:2080-6.
22. Guo J, Hawwari A, Li H, Sun Z, Mahanta SK, Littman DR, et al. Regulation of the TCRalpha repertoire by the survival window of CD4(+)CD8(+) thymocytes. *Nat Immunol* 2002;3:469-76.
23. Martin E, Treiner E, Duban L, Guerri L, Laude H, Toly C, et al. Stepwise development of MAIT cells in mouse and human. *PLoS Biol* 2009;7:e54.
24. Rowe JH, Stadinski BD, Henderson LA, de Bruin LO, Delmonte O, Lee YN, et al. Abnormalities of T-cell receptor repertoire in CD4(+) regulatory and conventional T cells in patients with RAG mutations: implications for autoimmunity. *J Allergy Clin Immunol* 2017;140:1739-43.e7.
25. Neven B, Perot P, Bruneau J, Pasquet M, Ramirez M, Diana JS, et al. Cutaneous and visceral chronic granulomatous disease triggered by a rubella virus vaccine strain in children with primary immunodeficiencies. *Clin Infect Dis* 2017;64:83-6.
26. Bednarski JJ, Sleckman BP. Lymphocyte development: integration of DNA damage response signaling. *Adv Immunol* 2012;116:175-204.
27. Eberhard JM, Hartjen P, Kummer S, Schmidt RE, Bockhorn M, Lehmann C, et al. CD161+ MAIT cells are severely reduced in peripheral blood and lymph nodes of HIV-infected individuals independently of disease progression. *PLoS One* 2014;9:e111323.
28. Magalhaes I, Pingris K, Poitou C, Bessoles S, Venteclef N, Kiaf B, et al. Mucosal-associated invariant T cell alterations in obese and type 2 diabetic patients. *J Clin Invest* 2015;125:1752-62.
29. Grimaldi D, Le Bourhis L, Sauneuf B, Dechartres A, Rousseau C, Ouaz F, et al. Specific MAIT cell behaviour among innate-like T lymphocytes in critically ill patients with severe infections. *Intensive Care Med* 2014;40:192-201.
30. Okada S, Markle JG, Deenick EK, Mele F, Averbuch D, Lagos M, et al. Impairment of immunity to *Candida* and *Mycobacterium* in humans with bi-allelic RORC mutations. *Science* 2015;349:606-13.
31. Griffith LM, Cowan MJ, Notarangelo LD, Kohn DB, Puck JM, Shearer WT, et al. Primary Immune Deficiency Treatment Consortium (PIDTC) update. *J Allergy Clin Immunol* 2016;138:375-85.
32. Plowman PN, Bridges BA, Arlett CF, Hinney A, Kingston JE. An instance of clinical radiation morbidity and cellular radiosensitivity, not associated with ataxia-telangiectasia. *Br J Radiol* 1990;63:624-8.
33. Riballo E, Critchlow SE, Teo SH, Doherty AJ, Priestley A, Broughton B, et al. Identification of a defect in DNA ligase IV in a radiosensitive leukaemia patient. *Curr Biol* 1999;9:699-702.

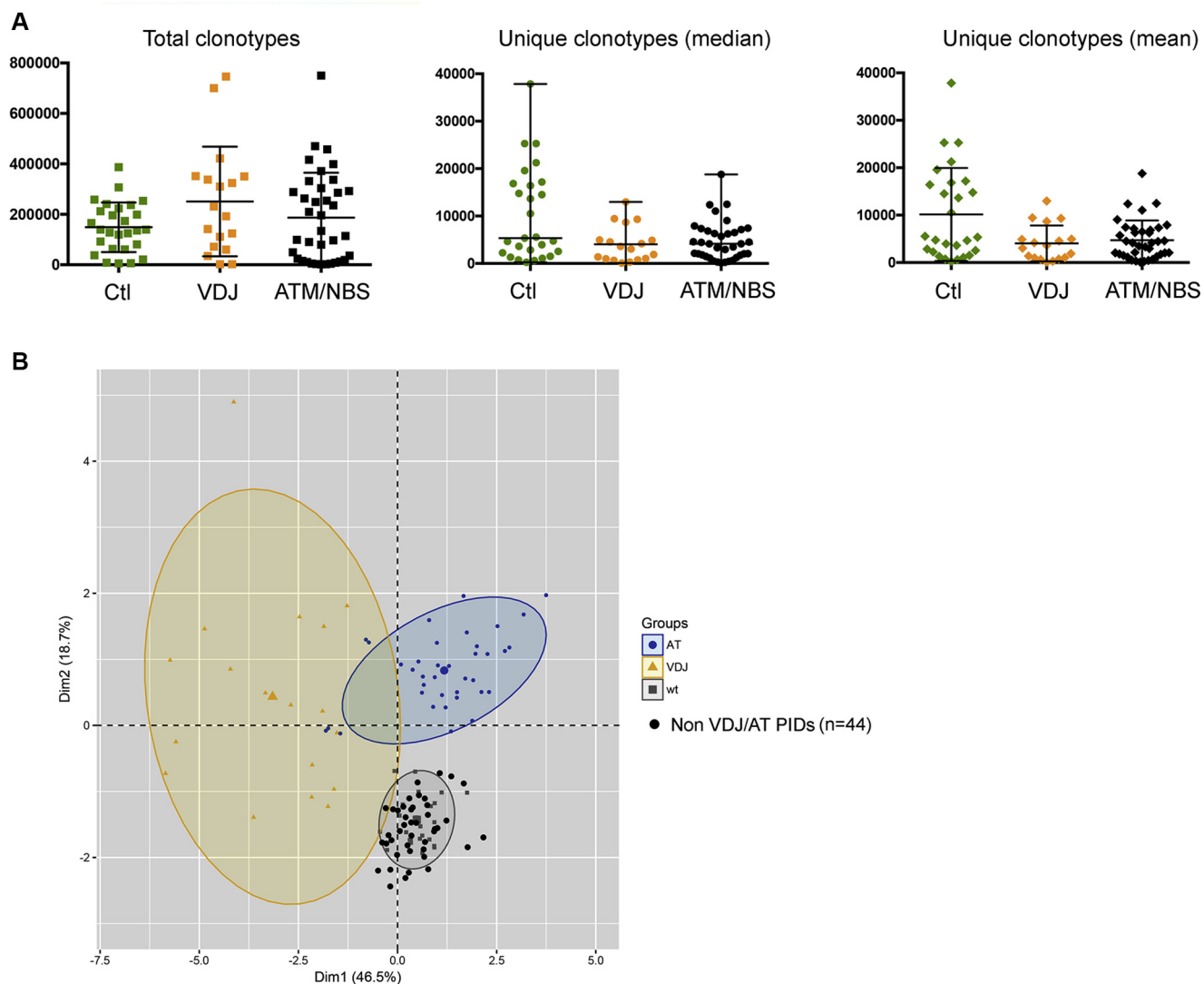


**FIG E1. A,** Metrics of PGM sequencing runs showing total numbers of identified clonotypes and medians and means of unique clonotypes among various samples. **B,** Forty-four non-VDJ or AT/PID patients (*black square*) clustered within the control group, attesting for specificity of the PROMIDIS $\alpha$  signature for VDJ patients and patients with AT.

**TABLE E1.** Genotypes of VDJ-deficient patients, patients with AT, and patients with NBS

Patients	Gene	Allele no. 1		Allele no. 2	
		Nucl	Prot	Nucl	Prot
VDJ					
NHEJ1	<i>Cernunnos/Xlf</i>	c.177del	p.E60Sfs*1	hmz	
NHEJ2	<i>Cernunnos/Xlf</i>	c.177del	p.E60Sfs*1	hmz	
NHEJ3	<i>Cernunnos/Xlf</i>	c.532C>T	p.R178*	hmz	
NHEJ4	<i>Cernunnos/Xlf</i>	c.532C>T	p.R178*	hmz	
NHEJ5	<i>Lig4</i>	c.2440C>T	p.R814*	c.1270_1274del	p.K424Rfs*20
NHEJ6	<i>Lig4</i>	c.833G>A	p.R278H	c.1271_1275del	p.K424Rfs*21
RAG1†	<i>RAG1</i>	c.1123C>G	p.H375D	c.1228C>T	p.R410W
NHEJ7†	<i>DCLER1C/Artemis</i>	c.500C>T	p.T167M	c.58G>C	p.D20H
RAG2†	<i>RAG1</i>	c.2446 G>A	p.G816R	hmz	
NHEJ8†	<i>PRKDC/DNAPKcs</i>	c.9185T>G	p.L3062R	hmz	
NHEJ9	<i>Lig4</i>	c.875A>G	p.Q292R	c.1307_1311del	p.K436Rfs*20
NHEJ10	<i>DCLER1C/Artemis</i>	Complex (insertion 196-bp mitochondrial DNA and large genomic deletion spanning exon 2)			
RAG3	<i>RAG1</i>	c.1420C>T	p.R474C	c.2304C>A	p.Y768*
NHEJ11	<i>PRKDC/DNAPKcs</i>	c.9185T>G	p.L3062R	hmz	
NHEJ12	<i>DCLER1C/Artemis</i>	c.19C>T	p.Q7*	c.58G>C	p.D20H
NHEJ13	<i>DCLER1C/Artemis</i>	c.1290_1306del	p.T432Sfs*16	hmz	
RAG4†	<i>RAG1</i>	c.1420C>T	p.R474C	c.2753_2755del	p.R918_F919delinsL
NHEJ14	<i>DCLER1C/Artemis</i>	c.1290_1306del	p.T432Sfs*16		
AT					
AT1	<i>ATM</i>	c.513C>T	p.Y171Y	c.3383A>G	p.Q1128R
AT2	<i>ATM</i>	c.496+3A>C	Predicted skipping exon 6	c.3756_3757dupTA	p.K1253Ilefs*5
AT3	<i>ATM</i>	c.496+3A>C	Predicted skipping exon 5	c.3756_3757dupTA	p.K1253Ilefs*4
AT4	<i>ATM</i>	c.850C>T	p.Q284X	c.6203T>C	p.L2068S
AT5	<i>ATM</i>	c.4634T>A	p.L1545*	c.9022C>T	p.R3008C
AT6	<i>ATM</i>	c.3085dupA	p.T1029Nfs*19	del Ex21-29	
AT7	<i>ATM</i>	c.103C>T	p.R35*	c.2413C>T	p.R805*
AT8	<i>ATM</i>	del Ex17-29		hmz	
AT9	<i>ATM</i>	c.9161C>T	p.A3054V	hmz	
AT10	<i>ATM</i>	c.5712dupA	p.S1905Ifs*25	hmz	
AT11	<i>ATM</i>	IVS19+02T>G		IVS25+32_34delCAT	
AT12	<i>ATM</i>	c.2921+1G>A	Skip exon 19	c.7927+5del	Skip exon 53
AT13	<i>ATM</i>	c.2135C>G	p.S712*	hmz	
AT14	<i>ATM</i>	c.790delT	p.275*	c.3712del5	p.1243*
AT15	<i>ATM</i>	c.7456C>T	p.R2486*	c.8161G>A	p.D2721N
AT16	<i>ATM</i>	c.7456C>T	p.R2486*	c.8161G>A	p.D2721N
AT17	<i>ATM</i>	c.491_492insT	p.184*	hmz	
AT18	<i>ATM</i>	c.491_492insT	p.184*	hmz	
AT19	<i>ATM</i>	8781_8785+2del	p.F2927Lfs*4	hmz	
AT20	<i>ATM</i>	c.3894dup	p.A1299Cfs*3	c.7630-2A>C	p.L2544Nfs*23
AT21	<i>ATM</i>	c.6383dupT	p.L2128Ffs*18	c.8395_8404del10	F2799Kfs*4
AT22	<i>ATM</i>	c.5441dup	p.L1814Ffs*9	del Ex30-32	
AT23	<i>ATM</i>	c.5415G>A	p.W1805*	c.7456C>T	p.R2486*
AT24	<i>ATM</i>	c.967A>G	p.I323V	hmz	
AT25	<i>ATM</i>	c.1564_1565delAG	p.Q522Ifs*43	IVS10-6T>G	
AT26	<i>ATM</i>	c.1960C>T	p.Q654*	c.3802delG	p.V1268*
AT27†	<i>ATM</i>	c.3894dupT	p.A1299Cfs*	?	
AT28†	<i>ATM</i>	deletion exons 17 to 29		hmz	
AT29	<i>ATM</i>	c.103C>T	p.R35*	hmz	
AT30	<i>ATM</i>	c.271C>T	p.Q91*	c.6453-1_6457del	?
AT31	<i>ATM</i>	c.7788G>A	Skip exon 52	c.6188G>A	p.G2063E
AT32	<i>ATM</i>	c.1711dup	p.S571Ffs*18	c.7876G>A	p.A2626T
AT33†	<i>ATM</i>	c.967A>G	p.I323V	hmz	
AT34†	<i>ATM</i>	c.967A>G	p.I323V	hmz	
AT35†	<i>ATM</i>	c.5497-2A>C	p.?	c.7090-19_c.7090-18ins(6019)	p?
AT36†	<i>ATM</i>	c.5497-2A>C	p.?	c.7090-19_c.7090-18ins(6019)	p?
AT37	<i>ATM</i>	c.3712_3716del	p.L1238Kfs*6	c.9139C>T	p.R3047*
NBS					
NBS2	<i>NBN</i>	c.657-661del	p.K219Nfs*16	hmz	
NBS3	<i>NBN</i>	c.657-661del	p.K219Nfs*16	hmz	
NBS1†	<i>NBN</i>	c.657-661del	p.K219Nfs*16	hmz	

NHEJ, Nonhomologous DNA end-joining.

†Prospective analysis.